Equivalent-Circuit Model for Axisymmetric High-Temperature Superconducting Film: Application to Contactless jC Measurement System and Pellet Injection System

Equivalent-Circuit Model for Axisymmetric High-Temperature Superconducting Film: Application to Contactless j_{C} Measurement System and Pellet Injection System

Takazumi Yamaguchi[1], Teruou Takayama[2], Atsushi Kamitani[2], and Hiroaki Ohtani[1,3]
[1]SOKENDAI (The Graduate University for Advanced Studies), Toki, Gifu 509-5292, Japan
[2]Yamagata University, Yonezawa, Yamagata 992-8510, Japan
[3]National Institute for Fusion Science, Toki, Gifu 509-5292, Japan

By using an equivalent-circuit model, a shielding current density in an axisymmetric high-temperature superconducting (HTS) film can be analyzed. In the present study, this model is applied to a permanent magnet method, inductive method, and pellet injection system in order to investigate their performance. As a result, it became clear that the inductive method can estimate a critical current density with an error less than 7%. Moreover, the permanent magnet method can be applied to the HTS film having a critical current density from 0.1 MA/cm^2 to 10 MA/cm^2. The numerical result also shows that a mass of HTS film can be reduced to about 40% without deteriorating an acceleration performance of the pellet injection system.

***Index Terms*—Critical current density, equivalent circuits, high-temperature superconductors, numerical simulation.**

I. Introduction

A high-temperature superconducting (HTS) film is used for numerous engineering devices. The analysis of the shielding current density in the HTS is essential to develop the HTS devices. By using the equivalent-circuit model (ECM) [1], the analysis of the shielding current density becomes equivalent to solving the initial-value problem of the 1st-order ordinary differential system.

The accurate measurement of the critical current density j_{C} is also required for the development of the HTS devices. As a contactless j_{C} measurement system, the permanent magnet method [2] and the inductive method [3] are widely used. In these methods, the HTS film is exposed to the dc/ac magnetic field. Therefore, the analysis of the shielding current density is required to measure the accuracy of these methods.

On the other hand, a superconducting linear acceleration (SLA) system [4], [5] has been recently proposed as an alternative pellet injection system for the fusion reactor. The pellet is accelerated by the Lorentz force acting on the ring-shaped HTS film, and the SLA system can inject it into the core plasma. By analyzing the shielding current density in the ring-shaped film, the acceleration performance of the SLA system is investigated numerically.

The purpose of the present study is to verify that the ECM can be applied to the simulations of the HTS devices. Moreover, the performances of the contactless j_{C} measurement systems and the SLA system are investigated by the ECM.

II. Equivalent-Circuit Model

Throughout the present study, we assume that the HTS film is axisymmetric. The HTS film of thickness b, inner radius R_{in}, and outer radius R_{out} is shown in Fig. 1 (a). If the inner radius is assumed as $R_{\mathrm{in}} = 0$, the HTS film is disk-shaped. The HTS film is exposed to the axisymmetric magnetic flux density generated by the cylindrical electromagnet/coil. Under the above assumption, the distribution of the shielding current density in the HTS film can be approximated as a set of multiple current loops, $\Lambda_1, \Lambda_2, \cdots, \Lambda_n$ (see Fig. 1 (b)). Here, Λ_i is the i-th current loop of radius r_i which has a cross section of width Δr_i and thickness b. In addition, the electric current and voltage in Λ_i are denoted by I_i and V_i, respectively.

By using the above assumption, the time evolution of the shielding current density is governed by the following circuit equation:

$$L\frac{d\boldsymbol{I}}{dt} = -\left[\frac{d}{dt}\left(\boldsymbol{M}(Z)I_{\mathrm{coil}}\right) + \boldsymbol{V}\right], \tag{1}$$

where $\boldsymbol{I} \equiv [I_1, I_2, \cdots, I_n]^T$, $\boldsymbol{V} \equiv [V_1, V_2, \cdots, V_n]^T$, and $\boldsymbol{M} \equiv [M_1(Z), M_2(Z), \cdots, M_n(Z)]^T$. Also, I_{coil} denotes the dc/ac current in the electromagnet/coil, and $M_i(Z)$ is a mutual inductance by the electromagnet/coil on Λ_i. Furthermore, Z is a position of the HTS film. Moreover, L is an inductance matrix, and its (i, j) entry shows an inductance by Λ_j on Λ_i.

In addition, the induced voltage V_i is determined by the power law [6]:

$$V_i = V_{\mathrm{C}i}\left(\frac{|I_i|}{I_{\mathrm{C}i}}\right)^N \mathrm{sgn}(I_i), \tag{2}$$

where $V_{\mathrm{C}i} \equiv 2\pi(r_i + \Delta r_i/2)E_{\mathrm{C}}$ and $I_{\mathrm{C}i} \equiv j_{\mathrm{C}} b \Delta r_i$. Here, E_{C} and j_{C} denote the critical electric field and the critical current density, respectively. In addition, N is a positive constant.

The circuit equation (1) with the power law (2) governs the time evaluation of the shielding current density in the axisymmetric HTS film. Note that the shielding current in the ring-shaped HTS film can be analyzed easily by assuming $R_{\mathrm{in}} > 0$.

Corresponding author: Takazumi Yamaguchi (email: yamaguchi.takazumi@nifs.ac.jp).

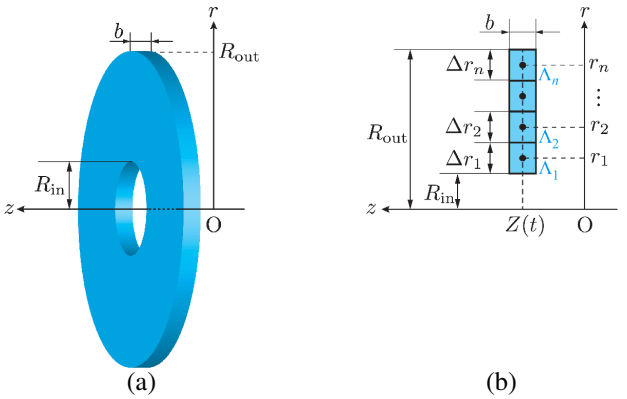

Fig. 1. (a) An axisymmetric HTS film and (b) a set of multiple current loops.

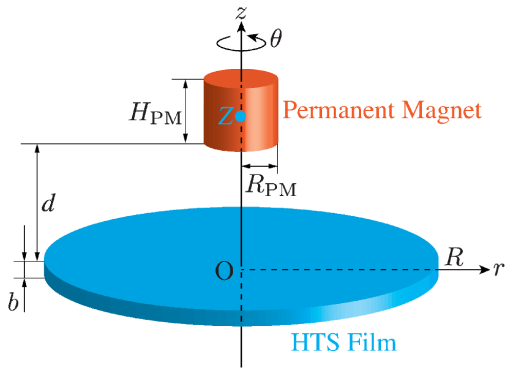

Fig. 2. A schematic view of the permanent magnet method.

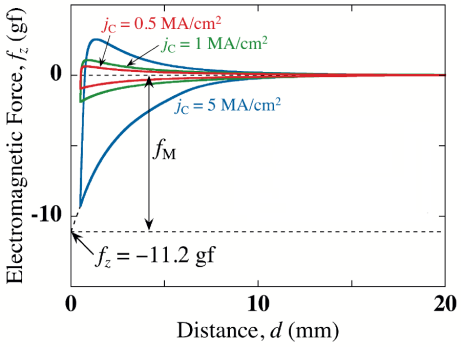

Fig. 3. Dependence of the electromagnetic force f_z on the distance d.

III. Simulation of Permanent Magnet Method

A. Permanent Magnet Method

A schematic view of the permanent magnet method is shown in Fig. 2. Throughout Section III, the shape of the HTS film is a disk of radius R and thickness b. Moreover, the cylindrical permanent magnet of radius $R_{\rm PM}$ and height $H_{\rm PM}$ is placed just above the HTS film. In this method, the permanent magnet first approaches the HTS film at constant speed for $0 \le t \le \tau_0$. Subsequently, the permanent magnet is kept away from the HTS film at the same speed for $\tau_0 < t \le 2\tau_0$. The position of the permanent magnet is $Z(t)$, and the distance between the HTS film and the permanent magnet denotes $d(t)$. In addition, the maximum and the minimum distance are denoted by $d_{\rm max}$ and $d_{\rm min}$, respectively. Also, we assume that the permanent magnet generates the magnetic flux density $B_{\rm T}$. Here, $B_{\rm T}$ is the magnetic flux density at $(r, z) = (0, b/2)$ when $d = d_{\rm min}$ is satisfied.

For the purpose of using the ECM, the permanent magnet is approximated as the electromagnet of the same radius and height. In addition, the steady-state current $I_{\rm coil}$ flows in the electromagnet. The electromagnet does not have thickness. Under the above assumption, the time dependence of the shielding current $\boldsymbol{I}(t)$ is governed by (1). By solving (1) with an initial condition, $\boldsymbol{I} = \boldsymbol{0}$ at $t = 0$, we can determine the shielding current $\boldsymbol{I}(t)$. Throughout the present study, the 5th-order Runge-Kutta method with the adaptive step-size control algorithm [7], [8] is applied to the initial-value problem such as (1). The numerical instability can be suppressed by using the adaptive step-size control algorithm.

The critical current density $j_{\rm C}$ is estimated from the Lorentz force acting on the HTS film. Once the initial-value problem is solved, we can determine z-component of the Lorentz force f_z easily.

B. Comparison with Experimental Result

Let us compare the result obtained by the ECM with that obtained by the experiment. In Section III, the geometrical and the physical parameters are fixed as follows: $R_{\rm PM} = 2.5$ mm, $H_{\rm PM} = 3$ mm, $d_{\rm max} = 20$ mm, $d_{\rm min} = 0.2$ mm, $\tau_0 = 39$ s, $B_{\rm T} = 0.3$ T, $R = 10$ mm, $b = 600$ nm, $N = 16$, and $n = 600$.

First, the dependence of the Lorentz force f_z on the distance d is shown in Fig. 3. According to this figure, the repulsive force increases as the permanent magnet approaches the HTS film. In addition, the absolute Lorentz force $|f_z|$ increases with the critical current density $j_{\rm C}$. Here, the maximum repulsive force $f_{\rm M}$ is defined as the Lorentz force $|f_z|$ at $d = 0$. For the case with $j_{\rm C} = 5$ MA/cm^2, $f_{\rm M}$ is 11.2 gf.

Next, Fig. 4 shows the dependence of the maximum repulsive force $f_{\rm M}$ on the critical current density $j_{\rm C}$. The maximum repulsive force $f_{\rm M}$ increases in proportion to the critical current density $j_{\rm C}$. In addition, Fig. 4 shows the maximum repulsive force $f_{\rm M}$ obtained by the experiment [2]. The proportional relationship of the ECM is qualitatively equal to the experimental result. However, the simulation result is not quantitatively equal to the experimental result. Because the HTS film used in the experiment contains tiny cracks and/or the crystal grain, (2) does not strictly govern the I–V characteristics.

IV. Simulation of Inductive Method

A. Inductive Method

A schematic view of the inductive method is shown in Fig. 5. The $N_{\rm c}$–turn coil in which the ac current $I_{\rm coil}(t) = I_0 \sin 2\pi f t$ flows is placed just above the HTS film. The inner and the outer radius of the coil are denoted by R_1 and R_2, respectively. Moreover, z-coordinate of the lower and the upper surface are represented by Z_1 and Z_2, respectively. As

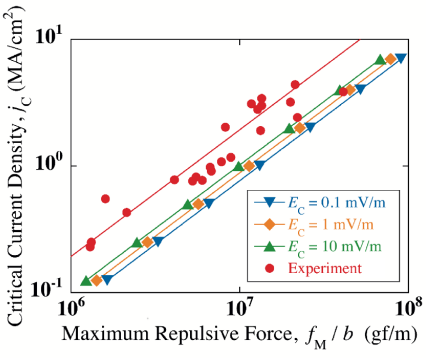

Fig. 4. Dependence of the maximum repulsive force $f_{\rm M}$ on the critical current density $j_{\rm C}$.

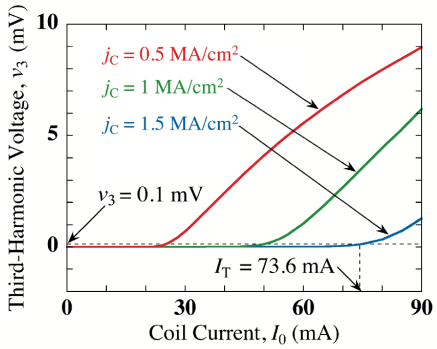

Fig. 6. The third-harmonic voltage v_3 as functions of the amplitude I_0.

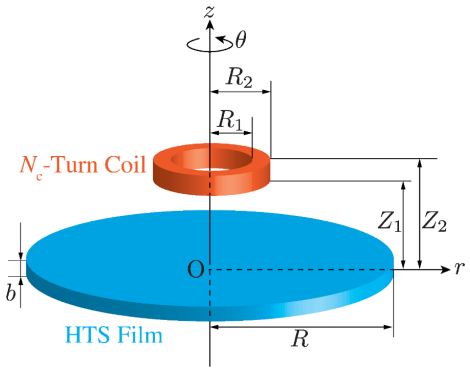

Fig. 5. A schematic view of the inductive method.

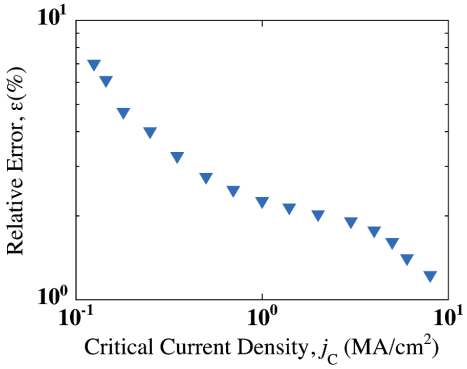

Fig. 7. Dependence of the relative error ε on the critical current $j_{\rm C}$.

in Section III, we assume that the shape of the HTS film is a disk of radius R and thickness b.

In the inductive method, the critical current density $j_{\rm C}$ is estimated from the threshold current $I_{\rm T}$. If and only if the amplitude I_0 exceeds the threshold current $I_{\rm T}$, the induced voltage v in the coil contains the third-harmonic voltage v_3. We can estimate $j_{\rm C}$ from $I_{\rm T}$ by means of the following equation:

$$j_{\rm C} = \frac{2F(r_{\rm max})I_{\rm T}}{b}, \tag{3}$$

where $F(r_{\rm max})$ denotes the maximum of the primary coil-factor function $F(r)$ [3].

The threshold current $I_{\rm T}$ can be determined by the following four steps:

1) The initial-value problem of (1) is solved with the initial condition, $\boldsymbol{I} = \boldsymbol{0}$ at $t = 0$, to obtain $\boldsymbol{I}(t)$. After that, the magnetic flux $\Phi(t)$ linked in the coil is calculated from $\boldsymbol{I}(t)$.
2) The third-harmonic voltage v_3 is determined by applying the discrete Fourier transform to the sampled data of $v(\equiv -d\Phi/dt)$.
3) The relationship between v_3 and I_0 is determined as the function of I_0. In order to determine $I_{\rm T}$, we adopt the voltage criterion [3]:

$$I_0 = I_{\rm T} \Longleftrightarrow v_3 = 0.1 \text{ mV}. \tag{4}$$

After determining $I_{\rm T}$ by the above steps, the critical current density is estimated by means of (3). In Section IV, the critical current density used for calculating (2) is denoted by $j_{\rm C}$, and the critical current density estimated by (3) is denoted by $j_{\rm C}^*$. In other word, $j_{\rm C}$ and $j_{\rm C}^*$ are the true critical current density and the current density obtained by the inductive method, respectively. In order to evaluate the accuracy, the relative error is defined as $\varepsilon \equiv |j_{\rm C} - j_{\rm C}^*|/|j_{\rm C}|$.

B. Accuracy of Inductive Method

Let us investigate the accuracy of the inductive method. In Section IV, the geometrical and the physical parameters are fixed as follows: $R_1 = 1$ mm, $R_2 = 2.5$ mm, $Z_1 = 0.2$ mm, $Z_2 = 1.2$ mm, $N_{\rm c} = 400$, $f = 1$ kHz, $R = 10$ mm, $b = 200$ nm, $E_{\rm C} = 1$ mV/m, $N = 16$, and $n = 1600$.

First, Fig. 6 shows the third-harmonic voltage v_3 as functions of the amplitude I_0. By applying (4) to this figure, $I_{\rm T}$ is estimated as follows: $I_{\rm T}$ = 24.6 mA, 49.2 mA, and 73.6 mA. Hence, $j_{\rm C}^*$ can be estimated as follows: $j_{\rm C}^* = 0.511$ MA/cm^2, 1.02 MA/cm^2, and 1.53 MA/cm^2.

Next, the dependence of the relative error ε on the critical current $j_{\rm C}$ is shown in Fig. 7 for investigating the accuracy of the inductive method. As is clear from this figure, the accuracy is improved with an increase in $j_{\rm C}$. Moreover, the error is less than 7% for the case with 0.1 MA/cm^2 $\leq j_{\rm C} \leq$ 10 MA/cm^2.

V. Simulation of SLA System

A. SLA system

A schematic view of the SLA system is shown in Fig. 8. A ring-shaped HTS film is attached to a pellet container. The

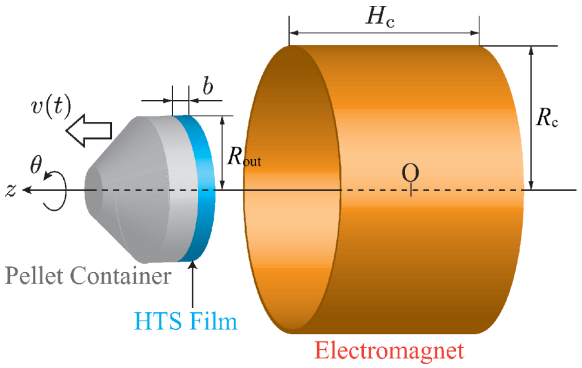

Fig. 8. A schematic view of the SLA system.

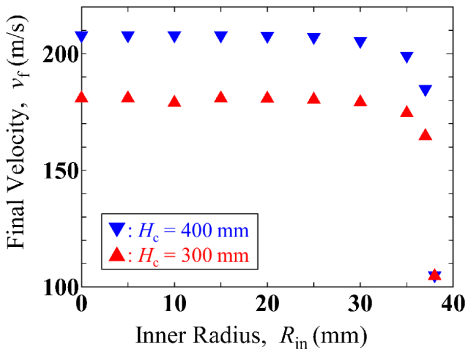

Fig. 9. Dependence of the final velocity v_f on the inner radius R_{in}.

inner radius, the outer radius, and the thickness of the HTS film are denoted by R_{in}, R_{out}, and b, respectively. Moreover, the HTS film is exposed to the magnetic flux density generated by the cylindrical electromagnet of height H_c and radius R_c. Furthermore, the coil current I_{coil} flowing in the electromagnet is controlled by the following equation:

$$I_{coil}(Z,t) = \begin{cases} \alpha t & (0 \le Z \le Z_{limit}) \\ 0 & (\text{otherwise}) \end{cases}, \tag{5}$$

where α is the increasing rate of the coil current. Also, the condition $0 \le Z \le Z_{limit}$ is the acceleration range.

Under the above assumption, the dynamic motion of the container is governed by the following Newton's equation of motion:

$$m\frac{d^2Z}{dt^2} = -2\pi \sum_{i=1}^{n} r_i B_r(r_i, Z, t) I_i, \tag{6}$$

where m is the total mass of the container and the HTS film. Also, $B_r(r,z,t)$ is r-component of the applied magnetic flux density. The time evolution of the shielding current and the dynamic motion of the container are governed by (6) coupled with (1). We can simulate the SLA system by solving the governing equation with the initial condition: $\boldsymbol{I} = \boldsymbol{0}$, $v = 0$, $Z = 1$ mm at $t = 0$.

B. Improvement of SLA system

Let us improve the acceleration performance of the SLA system by using the ring-shaped HTS film. In Section V, the geometrical and the physical parameters are fixed as follows: $R_c = 50$ mm, $\alpha = 20$ kA/ms, $Z_{limit} = 300$ mm, $R_{out} = 40$ mm, b =1 mm, N =20, $n = 400$, $E_C = 1$ mV/m, $j_C = 1$ MA/cm^2, and $m = 10$ g.

The dependence of the final velocity v_f on the inner radius R_{in} is shown in Fig. 9. The final velocity is the velocity at the time when $Z = Z_{limit}$ is satisfied. As shown in this figure, the inner radius R_{in} hardly influences the final velocity v_f for $R_{in} \lesssim 30$ mm. If the inner radius R_{in} is 30 mm, the mass of the HTS film is reduced to 40%. Therefore, the mass of the HTS film can be made light to improve the acceleration performance or to carry more fuel pellets.

VI. Conclusion

In order to verify that the ECM can be applied to the simulations of the HTS devices, we simulated the contactless j_C measurement systems and the SLA system. Conclusions are summarized as follows:

- The ECM can analyze the shielding current density in the ring-shaped HTS film without imposing the boundary condition. Furthermore, the ECM can be applied to the analysis of the shielding current density generated by the ac/dc magnetic field.
- The maximum repulsive force is completely proportional to the critical current density. This result is qualitatively equal to the experimental result. Therefore, the permanent magnet method is effective as a contactless j_C measurement system.
- The error of the inductive method is no more than 7%. In addition, the accuracy becomes high with an increase in a critical current density.
- By using the ring-shape HTS film, a total mass of the container can be made light. Hence, the acceleration performance of the SLA system can be improved.

References

[1] T. Yamaguchi, T. Takayama, A. Saitoh, and A. Kamitani, "Comparison between FEM and equivalent-circuit model simulations of superconducting linear acceleration system for pellet injection," *J. Adv. Simulat. Sci. Eng.*, vol. 4, no. 2, pp. 209-222, Aug. 2018.

[2] S. Ohshima, K. Takeishi, A. Saito, M. Mukaida, Y. Takano, T Nakamura, I. Suzuki, and M. Yokoo, "A simple measurement technique for critical current density by using a permanent magnet," *IEEE Trans. Appl. Supercond.*, vol. 15, no. 2, pp. 2911-2914, Jun. 2005.

[3] Y. Mawatari, H. Yamasaki, and Y. Nakagawa, "Critical current density and third-harmonic voltage in superconducting films," *Appl. Phys. Lett.*, vol. 81, no. 13 , pp. 2424-2426, Sep. 2002.

[4] N. Yanagi and G. Motojima, National Institute for Fusion Science, Toki, Gifu, private communication, 2017.

[5] T. Yamaguchi, T. Takayama, A. Saitoh, and A. Kamitani, "Numerical investigation on superconducting linear acceleration system for pellet injection by using equivalent-circuit model," *IEEE Trans. Magn.*, vol. 55, no. 6, Art. no. 7204305, June 2019.

[6] L. Makong, A. Kameni, P. Masson, J. Lambrechts, and F. Bouillault, "3-D modeling of heterogeneous and anisotropic superconducting media," *IEEE Trans. Magn.*, vol. 52, Art. no. 7205404, Mar. 2016.

[7] W. H. Press, S. A. Teukosky, W. T. Vetterling, and B. P. Flannery, "Numerical recipes in Fortran 77," *Cambridge Univ. Press.*, New York, USA, 1992.

[8] A. Kamitani, T. Takayama, and H. Nakamura, "High performance analysis of shielding current density in high temperature superconducting thin film," *Plasma Fusion Res.*, vol. 5, Art. no. S2112, Mar. 2010.